# $p$-ADAPTIVE BOUNDARY ELEMENTS FOR THREE-DIMENSIONAL POTENTIAL PROBLEMS

MIGUEL CERROLAZA

ENRIQUE ALARCÓN

## INTRODUCTION

The BEM has generated a great deal of scientific research and engineering applications in the past, in an attempt to take advantage of the reduction of input data in three-dimensional problems (only the boundary needs to be discretized). From another point of view, $p$-convergence in the finite element method (FEM) gives very good results. This suggests the possibility of applying the same approach to the BEM,[1–3] opening up an interesting new area on the implementation of numerical methods and the establishment of suitable convergence criteria.

This paper extends the $p$-convergence in the BEM to three-dimensional problems and discusses in detail some previously presented convergence criteria related to the BEM method.

Numerical results from illustrative examples are apparently good enough and ensure the possibility of treating more complicated problems with the same technique.

## HIERARCHICAL INTERPOLATION FUNCTIONS

The first step of the method is the choice of the interpolation family functions. Our criterion is to select the largest boundary elements compatible with both geometry and boundary condition discontinuities. This choice minimizes the number of boundary elements and, of course, the operations required in the analysis procedure.

Next, the hierarchy of the interpolation functions to be used in the successive approximations process is defined. In previous papers dealing with plane potential problems the Peano's family was used.[4] In those cases it was observed that for high-order polynomial degree the convergence rate was slower than for low degrees. Although that problem deserves more research, in this paper we have decided to change to the Legendre family of interpolation functions, defined by

$$P_p(\xi) = \frac{1}{(p-1)!}\frac{1}{2^{p-1}}\frac{\mathrm{d}^p}{\mathrm{d}\xi^p}[(\xi^2-1)^p] \tag{1}$$

with appropriate combinations based on the well-known tensorial products.[5,9]

These functions are defined over either edges or elements, requiring a careful strategy when programming the adaptive process in order to consider the respective refinements in a sequential way.

## COLLOCATION POINTS

As is well known, BEM integral equations are generated by collocating the fundamental solution (Green's function for the whole space) in selected boundary points. In the particular case of the isoparametric BEM, the same set of points to define geometry, boundary conditions, interpolation points and collocation points is used, thus producing undesirable effects when the method must fit into special local situations.

However, in the BEM $p$-adaptive version we have complete freedom for selecting nodal points. The main idea is to choose the collocation points where the interpolation functions give their maximum value, in order to reinforce the corresponding dominant element within the influence matrix. Also, collocation points must be placed as far apart as possible to avoid ill-conditioning in the system of equations. Thus, bilinear functions are defined in corner nodes and odd/even functions are defined in nodes belonging to edges/elements, respectively.

Searching for the best place to define collocation points and its importance in the context of the BEM $p$-convergence approach is an open question.

## GEOMETRY REPRESENTATION AND BOUNDARY CONDITIONS

In the BEM $p$-adative approach, the geometry and boundary condition representations are independent of the process of analysis, allowing the use of geometry pre-processors in order to minimize error sources derived from non-regular discretizations.

The present development uses 'serendipity' functions, defined over double-curved variable-number-nodes surface elements to adjust both geometry and boundary conditions in an independent way.

'Self-solvable' corners and edges, produced by special boundary conditions, are identified and treated separately from the global process, reducing the number of operations required to reach the final solution.

## SOLUTION REFINEMENT: ADAPTIVE PROCESS

Once both geometry and boundary conditions are specified, the system produces a first solution based on bilinear interpolation for all unknown variables (i.e. potential and flux where applicable). In most cases, this solution is an acceptable one.

However, in general, it is necessary to refine the solution in certain boundary zones; this is done adding Legendre interpolation functions (1) sequentially.[6,7]

Edges and/or elements where refinement is necessary are selected with local indicators, calculated as follows.

## LOCAL INDICATORS

Problems governed by the Laplace equation are described by the representation formula

$$C\,\phi(P) + \int_{\partial\Omega} \phi(Q)\, q^*(P,Q) = \int_{\partial\Omega} q(Q)\phi^*(P,Q) \tag{2}$$

where $\Phi$ and $q$ are potential and flux fields, respectively, generated at $Q$ (boundary point) when the Laplace equation fundamental solution is located at $P$ (also boundary point). $C$ is a constant depending on boundary geometry at $P$.

The boundary $\Omega$ is, in general, divided into two regions:

$$\begin{aligned} &\partial\Omega_1\colon\ \phi = \phi^o \quad q = ? \\ &\partial\Omega_2\colon\ \phi = ? \quad q = q^o \end{aligned} \tag{3}$$

Thus, equation (2) becomes

$$C\,\phi(P) + \int_{\partial\Omega_2} \phi(Q).q^*(P,Q) - \int_{\partial\Omega_1} q(Q).\phi^*(P,Q) = -\int_{\partial\Omega_1} \phi^o(Q).q^*(P,Q) + \int_{\partial\Omega_2} q^o(Q).\phi^*(P,Q) \tag{4}$$

or, collecting terms

$$L_1\,q(P) + L_2\,\phi(P) + p(P) = 0 \tag{5}$$

where we state the following definition:

*Definition 1*

$$L_1 f(P) = 2\int_{\partial\Omega_1} f(Q)\,\phi^*(P,Q)$$

$$L_2 f(P) = C f(P) + \int_{\partial\Omega_2} f(Q) q^*(P,Q) \tag{6}$$

$$\mathrm{p(P)} = \int_{\partial\Omega_1} f^o(Q) q^*(P,Q) - \int_{\partial\Omega_2} \frac{\partial f}{\partial n}\bigg|_Q^o \phi^*(P,Q)$$

Unknown potential and flux are approximated over $\partial\Omega_2$ and $\partial\Omega_1$, respectively, through

$$\begin{aligned} \phi \sim \hat{\phi} &= a_1 N_1 + a_2 N_2 + \ldots + a_n N_n \quad \text{on} \quad \partial\Omega_2 \\ q \sim \hat{q} &= b_1 N_1 + b_2 N_2 + \ldots + b_n N_n \quad \text{on} \quad \partial\Omega_1 \end{aligned} \tag{7}$$

where $a_j$ and $b_j$ are parameters to be determined, whereas $N_j$ are elements of hierarchical family functions.

From these approximations, two errors are derived:

$$\begin{aligned} e_1 &= q - \hat{q} \quad \text{on } \partial\Omega_1; \quad e_1 = 0 \quad \text{on} \quad \partial\Omega_2 \\ e_2 &= \phi - \hat{\phi} \quad \text{on } \partial\Omega_2; \quad e_2 = 0 \quad \text{on} \quad \partial\Omega_1 \end{aligned} \tag{8}$$

The 'residual' $r$ is obtained by substituting (7) into (4):

$$r = L_1\,\hat{q} + L_2\,\hat{\phi} + p \tag{9}$$

It must be emphasized that residual $r$ is zero at collocation points and, with (9), $r$ can be calculated at any other boundary point.[6]

From (8) we can write

$$\begin{aligned} L_1\,\hat{q} &= L_1\,q - L_1\,e_1 \\ L_2\,\hat{\phi} &= L_2\,\phi - L_2\,e_2 \end{aligned} \tag{10}$$

Thus, $r$ becomes

$$r = L_1\,q + L_2\,\phi + p - (L_1\,e_1 + L_2\,e_2) \tag{11}$$

and after some manipulations

$$L_1\,e_1 + L_2\,e_2 + r = 0 \tag{12}$$

or, in other words, residuals are 'loads' which 'equilibrate' errors. Finally, from (8),

$$\begin{aligned} &\text{On } \partial\Omega_1\text{:} \quad r = -L_1\,e_1 = r_1 \\ &\text{On } \partial\Omega_2\text{:} \quad r = -L_2\,e_2 = r_2 \end{aligned} \tag{13}$$

*Energy error*

Although the BEM approach is a collocation method, a global 'energy' error can be established through techniques resembling the Galerkin method:[8]

*Definition 2*

$$\|e\|_E^2 = \int_{\partial\Omega_1} e_1(L_1\,e_1) + \int_{\partial\Omega_2} e_2(L_2\,e_2) = -\int_{\partial\Omega_1} e_1\,r_1 - \int_{\partial\Omega_2} e_2\,r_2 \tag{14}$$

or, developing this definition further:

$$\|e\|_E^2 = \int_{\partial\Omega_1} e_1(P)\left[-\int_{\partial\Omega_1} e_1(Q)\phi^*(P,Q)\right] + \frac{1}{2}\int_{\partial\Omega_2}\left[e_2(P)\right]^2 + \int_{\partial\Omega_2} e_2(P)\left[\int_{\partial\Omega_2} e_2(Q).q^*(P,Q)\right] \tag{15}$$

where the term $\frac{1}{2}$ appears when integrating over $c^1$ boundaries. An interesting property of (14) is obtained considering that flux is known and potential is refined (potential is known and flux is refined), by adding a new interpolation function:

$$\begin{aligned} \phi \sim \hat{\hat{\phi}} &= \hat{\phi} + a_{n+1} N_{n+1} \\ (q \sim \hat{\hat{q}} &= \hat{q} + b_{m+1} N_{m+1}) \end{aligned} \tag{16}$$

or, substituting into (8),

$$\begin{aligned} e_2 = \phi - \hat{\phi} &\sim a_{n+1} N_{n+1} \\ (e_1 = q - \hat{q} &\sim b_{m+1} N_{m+1}) \end{aligned} \tag{17}$$

Now, using (14), we obtain

$$\|e\|_E^2 = -\, a_{n+1}\int_{\partial\Omega_2} N_{n+1}\, r_2 \tag{18}$$

$$(\|e\|_E^2 = -\, b_{m+1}\int_{\partial\Omega_1} N_{m+1}\, r_1)$$

It can be seen that the energy error is related to the dot product of $r$ and $N_{n+1}$. In fact, this error works to indicate the usefulness of introducing the new function but not to estimate the actual value of the residual. Now, it is possible to establish a relationship between error and residual.

With (17) and (13)

$$\begin{aligned} L_2 e_2 = a_{n+1} L_2 N_{n+1}\,;\, r_2 &= -\, a_{n+1} L_2 N_{n+1} \\ (L_1 e_1 = b_{m+1} L_1 N_{m+1}\,;\, r_1 &= -\, b_{m+1} L_1 N_{m+1}) \end{aligned} \tag{19}$$

Substituting into (18)

$$\|e\|_E^2 = a_{n+1}^2 \int_{\partial\Omega_2} N_{n+1} L_2 N_{n+1} \tag{20}$$

$$(\|e\|_E^2 = b_{m+1}^2 \int_{\partial\Omega_1} N_{m+1} L_1 N_{m+1})$$

Comparing (20) with (18) we note that

$$a_{n+1} = \frac{\displaystyle\int_{\partial\Omega_2} N_{n+1}\, r_2}{\displaystyle\int_{\partial\Omega_2} N_{n+1}\, L_2\, N_{m+1}} \tag{21}$$

$$\left(b_{n+1} = \frac{\displaystyle\int_{\partial\Omega_1} N_{m+1}\, r_1}{\displaystyle\int_{\partial\Omega_1} N_{m+1}\, L\, N_{m+1}}\right)$$

and substituting again into (20), we arrive at the desired expression for the indicator:

$$\|e\|_E^2 = \frac{\left[\displaystyle\int_{\partial\Omega_2} N_{n+1}\, r_2\right]^2}{\displaystyle\int_{\partial\Omega_2} N_{n+1}\, L_2\, N_{n+1}} \tag{22}$$

$$\left( \|e\|_E^2 = \frac{\left[ \int_{\partial\Omega_1} N_{m+1}\, r_1 \right]^2}{\int_{\partial\Omega_1} N_{m+1}\, L_1\, N_{m+1}} \right)$$

## GLOBAL ESTIMATORS

For each partial solution in the refinement process, it is necessary to determine the accuracy of the current solution. The development of a good global estimator is still an open question. However, in the particular case of a Neumann problem, the estimator takes the form

$$L_2\, e_2 = \int_{\partial\Omega_2} e_2(Q)\, q^*(P,Q) + C\, e_2(P) \tag{23}$$

If boundary elements are straight and, as usual, the collocation point belongs to the element

$$q^*(P,Q) = 0 \tag{24}$$

Therefore

$$r_2(P) = -L_2\, e_2 = -C\, e_2(P) \tag{25}$$

Substituting into (14)

$$\|e\|_E^2 = -\int_{\partial\Omega_2} e_2(P)\, r_2(P) = \frac{1}{C} \int_{\partial\Omega_2} r_2^2(P) \tag{26}$$

With $C=\frac{1}{2}$ and adding along the whole boundary

$$\|e\|_E^2 = 2 \sum \int_{\partial\Omega_i} r_2^2(P) \tag{27}$$

Equation (27) can also be used in the case of curved elements, if no other way is available.

Another estimator used in mixed problems is the summation of fluxes over the whole boundary, which must be zero. The magnitude of the 'desequilibrated' flux works as a parameter for stopping the refinement process when the previously defined accuracy is reached.

## NUMERICAL RESULTS: CONVERGENCE STUDY

In order to evaluate the convergence and the versatility of the numerical procedure developed, the BEM *p*-adaptive approach presented in the previous sections is now applied to two 3-D potential theory illustrative examples.

### *Hollow cylinder*

The temperature distribution in a hollow cylinder of internal/external radii equal to 4/10 and subjected to an internal/external temperature equal to 100/20 is studied. Figure 1(a) shows the geometry of a hollow cylinder wedge sector, whereas Figure 1(b) and 1(c) show the boundary conditions and potential theory solution, respectively.

This example was analysed using both the BEM *p*-refinement and *h*-refinement approaches. Figure 2 shows the logarithm evolution for the quadratic error proposed in expression (27), which is used as a global estimator for the solution convergence, versus the logarithm of $1/NDF$ ($NDF$ being the total number of integral equations at each refinement stage). Observe that *p*-refinement convergence (adaptive approach) is about 1·5 times faster than selective *h*-refinement convergence. This is a relevant and promising fact for future research.

Figure 3 shows the evolution of the summation of fluxes over the whole boundary (again in logarithm scale and squared to avoid the effect of sign), versus the logarithm of $1/NDF$. The *p*-

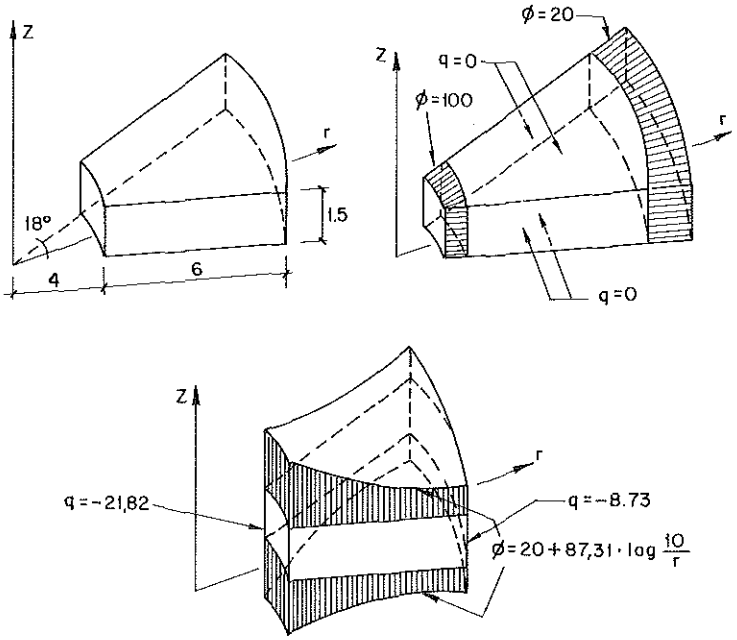


Figure 1. Hollow cylinder example: (a) geometry; (b) boundary conditions; (c) theoretical solution

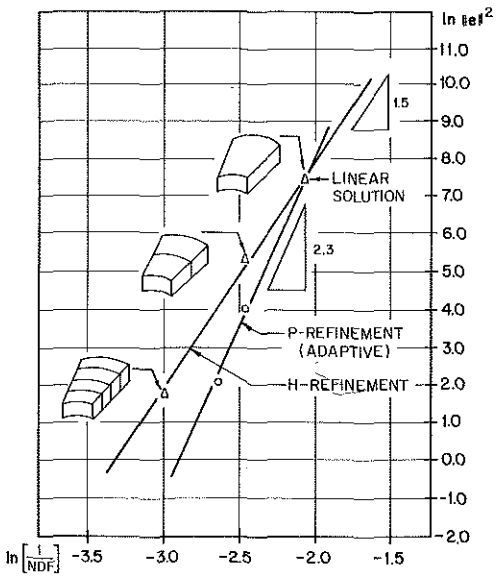


Figure 2. Residual error. Convergence rates in hollow cylinder analysis

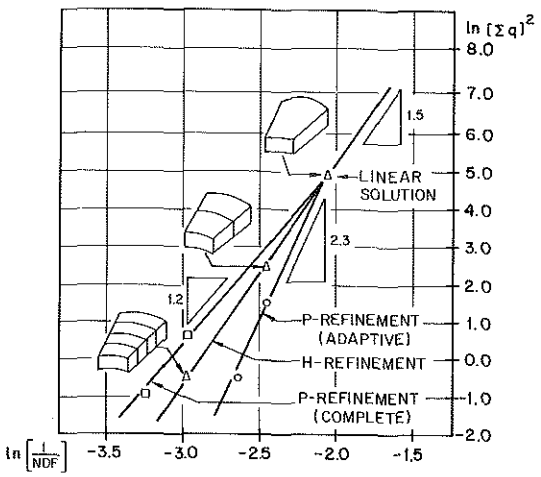


Figure 3. Summation of fluxes. Convergence rates in hollow cylinder analysis

refinement convergence (adaptive approach) is again faster than the $h$-refinement one. This figure points out the importance of using a local indicator. Observe that $p$-refinement convergence (complete approach) also ensures the convergence but, in this case, it is about 1·25 times slower than the selective $h$-refinement approach and 1·92 times slower than $p$-refinement convergence (adaptive approach). However, this kind of estimator must be used carefully because it could give wrong results when used over more complicated geometries.

*Pressure vessel*

A simplified wedge sector of an axially symmetric pressure vessel is now analysed to determine the temperature and flux fields over the boundary. The body geometry is 'extracted' from a parallelepiped body on which both exact solution and boundary conditions are known (see Figure 4).

Potential and flux fields are:

$$\phi = 3[x^2 - y^2] \tag{28}$$

$$q_x = \partial\phi/\partial x = 6x \tag{29}$$

$$q_y = \partial\phi/\partial y = -6y \tag{30}$$

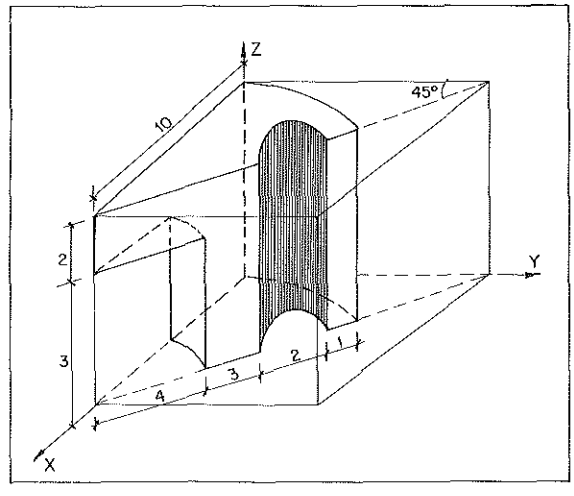


Figure 4. Axially symmetric pressure vessel 'extracted' from a parallelepipedic body

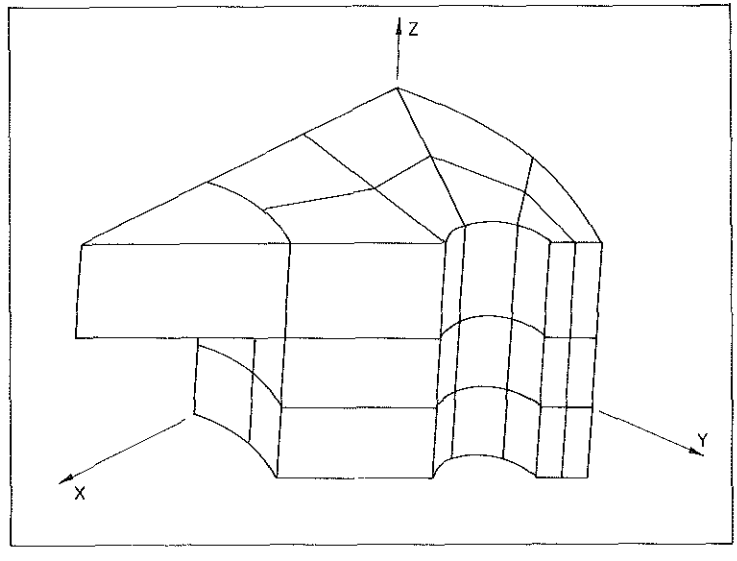


Figure 5. Pressure vessel: mesh A (82 nodes, 56 surface boundary elements)

In this way, it is possible to test the $p$-adaptive approach against the exact solution in three-dimensional solids with non-trivial geometries and using potential functions as complicated as necessary which must satisfy the Laplace equation.

This problem was analysed using bilinear interpolation functions over single-curved and plane surface quadrilateral variable-number-nodes elements, defining the meshes shown in Figures 5 and 6. Mesh A (Figure 5) was based on 82 nodes and 54 surface boundary elements, whereas mesh B (Figure 6) was based on 47 nodes and 29 surface boundary elements. Mesh C (Figure 7), used for the $p$-refinement approach, was defined with 28 nodes and 16 surface boundary elements.

Table I collects numerical comparisons and results obtained form various $p$-refinements over mesh C (Figure 7) and from bilinear interpolation over mesh A (Figure 5) for some critical points, also shown in Figure 7. The results show a very close agreement when compared with the theoretical solution as expected from $p$-refinement convergence (adaptive approach) to the exact solution.

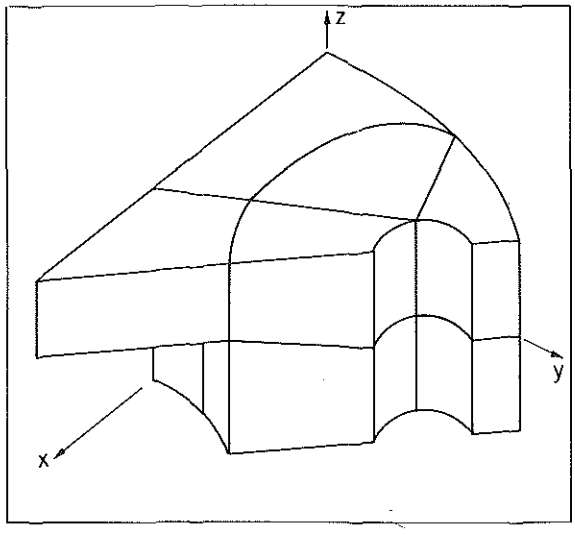


Figure 6. Pressure vessel: mesh B (47 nodes, 29 surface boundary elements)

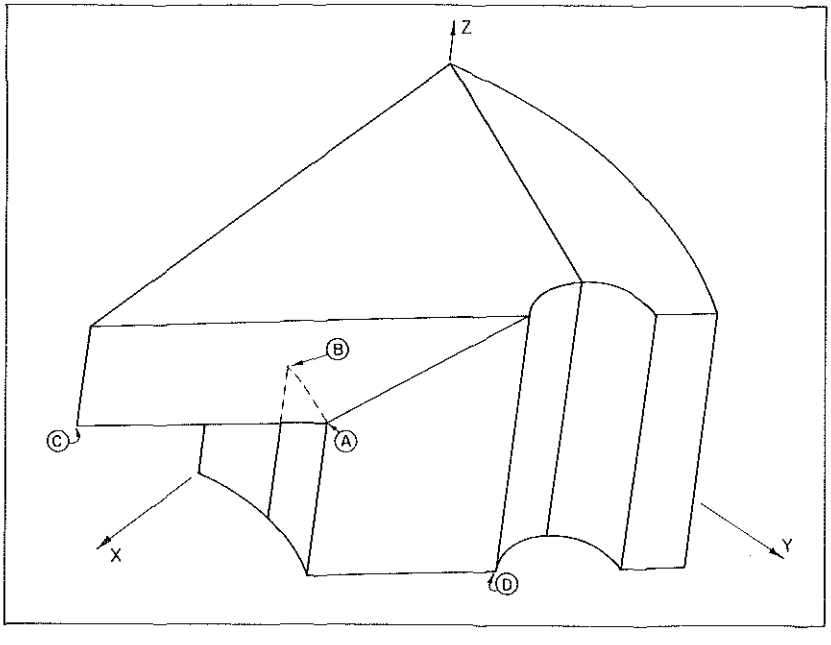


Figure 7. Pressure vessel: mesh C (28 nodes, 16 surface boundary elements). Some critical points marked with capital letters

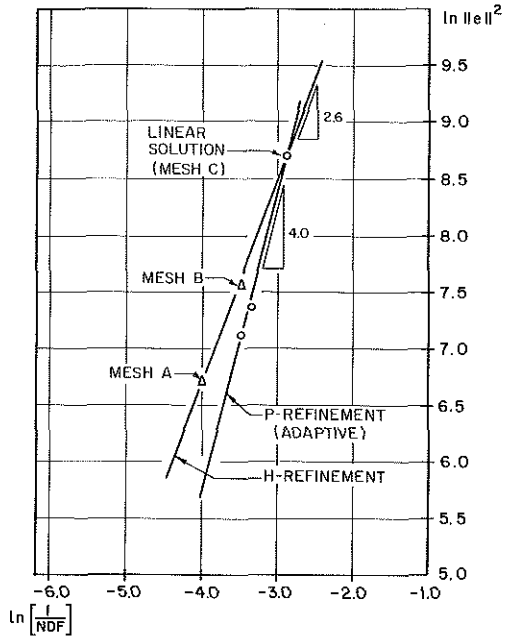


Figure 8. Global estimator convergence rates for pressure vessel analysis

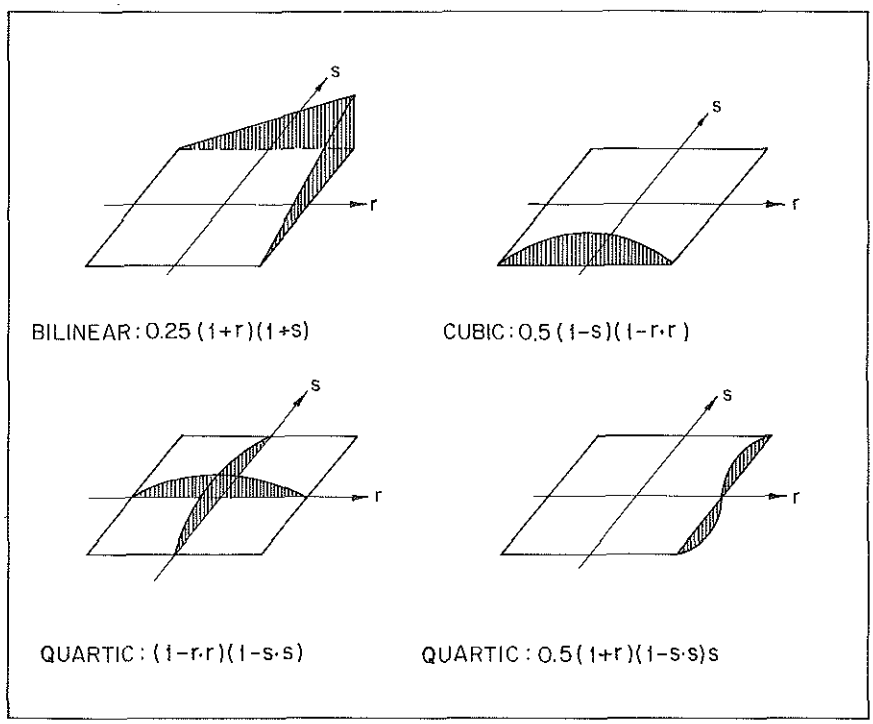


Figure 9. Some Legendre hierarchical interpolation functions for the non-dimensional space

Table I. Numerical comparisons between successive *p*-refinements and exact solution in the pressure vessel example

| | | Type of *p*-refinement† | | | | |
|---|---|---|---|---|---|---|
| Node | Variable | Bilinear | Cubic | Quartic | Mesh (Figure 5) | Theory |
| A | Pot. | 139·72 | 125·61 | 130·81 | 132·14 | 130·32 |
| B | Pot. | 123·96 | 106·93 | 112·65 | 114·06 | 112·20 |
| C | Pot. | 297·62 | 297·92 | 299·54 | 300·38 | 300·00 |
| D | Flux | −55·75 | −40·10 | −42·37 | −45·32 | −42·42 |
| No. of equations | | 18 | 41 | 52 | 56 | — |
| Boundary elements | | 16 | 16 | 16 | 54 | — |

† See Figure 9 for details.

Figure 8 illustrates the logarithmic evolution of the global estimator in expression (27), versus the logarithm of $1/NDF$, showing again that $p$-refinement convergence (adaptive approach) is faster than $h$-refinement convergence, even for more complicated non-smooth geometries.

## CONCLUSIONS

The $p$-adaptive approach for the analysis of three-dimensional potential problems, based on the BEM method, has been presented. Numerical results have demonstrated the suitability of the analytic procedure proposed here, showing that rates of $p$-convergence are faster than those of $h$-convergence.

The computer code developed in this research has a powerful geometric pre-processor for generating three-dimensional surfaces and offers the possibility of treating in an efficient way some critical numerical aspects associated with the BEM method: 'self-solution' corners and edges, high accuracy when integrating singular kernels, variable-number-nodes surface elements, etc.

Although the local indicators and global estimators proposed here have been used successfully, a large amount of research has to be done in the same direction for solving a great number of critical aspects, especially related to the reliability of the convergence criteria.


### ACKNOWLEDGEMENTS

This work has been produced as a part of a research plan promoted by the Comision Asesora de Investigacion Cïentífica y Tecnica (CAICYT).


### REFERENCES


1. E. Alarcon, L. Abia and A. Reverter, 'On the possibility of adaptive boundary elements', in *Accuracy Estimates and Adaptive Refinements in Finite Elements Computations (ARFEC)*, Lisbon, 1984.
2. E. Alarcon, A. Reverter and J. Molina, 'Hierarchical boundary elements', *Comp. Struct.*, **20**(1–3), 151–156 (1985).
3. E. Alarcon and A. Reverter, '*p*-Adaptive boundary elements', *Int. j. numer. methods eng.* **23**, 801–829 (1986).
4. A. G. Peano, 'Hierarchies of conforming finite elements', *Doctoral dissert.*, Washington Univ., St. Louis (1975).
5. K. Babuska and W. C. Rheinboldt, '*A posteriori* error estimates for the FEM', *Int. j. numer. methods eng.*, **12**, 1957–1616 (1978).
6. D. W. Kelly, J. Gago, O. C. Zienkiewicz and I. Babuska, '*A posteriori* error analysis and adaptive processes in the FEM', parts I and II, *Int. j. numer. methods eng.*, **19**, 1593–1619 (1983).
7. B. A. Szabo, P. K. Basu and M. P. Rosow, 'Adaptive finite element based on *p*-convergence', *NASA Conf. Pub. 2059*, pp. 43–50 (1978).
8. D. N. Arnold and W. L. Wendland, 'On the asymptotic convergence of collocation methods', *Preprint 665*, TH Darmstad, Dept. of Mathematics, Fed. Rep. Germany (1982).
9. I. Babuska, 'The selfadaptive approach in the FEM', in *Mathematics of Finite Elements and Applications* (J.R. Whiteman, Ed.), Academic Press, New York, 1975.